Title
Structural analysis of estrogen receptors: interaction between estrogen receptors and cav-1 within the caveolae

Journal
Biology of Reproduction, 100(2)

ISSN
0006-3363

Authors
Pastore, Mayra B
Landeros, Rosalina Villalon
Chen, Dong-bao
et al.

Publication Date
2019-02-01

DOI
10.1093/biolre/ioy188

Peer reviewed

Biology of Reproduction, 2019, 100(2), 495–504
doi:10.1093/biolre/ioy188
Research Article
Advance Access Publication Date: 23 August 2018

OXFORD

Research Article

Structural analysis of estrogen receptors: interaction between estrogen receptors and cav-1 within the caveolae†

Mayra B. Pastore [1,2], Rosalina Villalon Landeros [1], Dong-bao Chen [3] and Ronald R. Magness [1,4,*]

[1]Department of Obstetrics and Gynecology Perinatal Research Labs, University of Wisconsin-Madison, Madison, Wisconsin, USA; [2]Cellular and Molecular Pharmacology, University of California-San Francisco, San Francisco, California, USA; [3]Department of Obstetrics and Gynecology University of California Irvine, Irvine, California, USA and [4]Department of Obstetrics and Gynecology University of South Florida, Tampa, Florida, USA

*__Correspondence:__ Department of Ob/Gyn, Morsani College of Medicine, Perinatal Research Vascular Center, University of South Florida, 12901 Bruce B. Downs Blvd. MDC48 Tampa, FL 33612, USA. Tel: 813-974-8942; 608 417–9058; E-mail: rmagness@health.usf.edu

†__Grant Support:__ This work was supported by National Institutes of Health grants P01HD38843, R01s HL49210, HL87144, HL117341 (RRM), HL70562 (DC), R25-GM083252, 5T32-HD041921, and K12GM081266.
__Conference Presentation:__ Presented in part at the 46th Annual Meeting of the Society for the Study of Reproduction, July 22–26, 2013, Montreal, Quebec, Canada. Partial fulfillment of requirements of MBP for her PhD in the Endocrinology Reproductive Physiology training program.

Received 1 March 2018; Revised 13 August 2018; Accepted 20 August 2018

Abstract

Pregnancy is a physiologic state of substantially elevated estrogen biosynthesis that maintains vasodilator production by uterine artery endothelial cells (P-UAECs) and thus uterine perfusion. Estrogen receptors (ER-α and ER-β; ESR1 and ESR2) stimulate nongenomic rapid vasodilatory responses partly through activation of endothelial nitric oxide synthase (eNOS). Rapid estrogenic responses are initiated by the ~4% ESRs localized to the plasmalemma of endothelial cells. Caveolin-1 (Cav-1) interactions within the caveolae are theorized to influence estrogenic effects mediated by both ESRs. **Hypothesis:** Both ESR1 and ESR2 display similar spatial partitioning between the plasmalemma and nucleus of UAECs and have similar interactions with Cav-1 at the plasmalemma. Using transmission electron microscopy, we observed numerous caveolae structures in UAECs, while immunogold labeling and subcellular fractionations identified ESR1 and ESR2 in three subcellular locations: membrane, cytosol, and nucleus. Bioinformatics approaches to analyze ESR1 and ESR2 transmembrane domains identified no regions that facilitate ESR interaction with plasmalemma. However, sucrose density centrifugation and Cav-1 immunoisolation columns uniquely demonstrated very high protein–protein association only between ESR1, but not ESR2, with Cav-1. These data demonstrate (1) both ESRs localize to the plasmalemma, cytosol and nucleus; (2) neither ESR1 nor ESR2 contain a classic region that crosses the plasmalemma to facilitate attachment; and (3) ESR1, but not ESR2, can be detected in the caveolar subcellular domain demonstrating ESR1 is the only ESR bound in close proximity to Cav-1 and eNOS within this microdomain. Lack of protein–protein interaction between Cav-1 and ESR2 demonstrates a novel independent association of these proteins at the plasmalemma.

Summary Sentence

Since ESR1 and ESR2 plasma membrane location are respectively affiliated with Cav-1-dependent and Cav-1-indepenent mechanisms, a novel difference of ER regulation in endothelial cells derived from the uterine vasculature was identified.

Key words: estrogen receptors, ESR1, ESR2, ER-α, ER-β, Caveolae, pregnancy, nitric oxide, eNOS, uterine vasculature, endothelium.

Introduction

Normal pregnancy is characterized by a multitude of systemic and even more dramatic uterine vascular adaptations [1–6]. Specifically, uterine blood flow (UBF) increases from 1 to 2% of cardiac output during the nonpregnant state and reaches 15–25% of the elevated total cardiac output by term [1, 4, 7], which is necessary for the appropriate delivery of nutrient and oxygen to the placenta and thus the developing fetus [3, 4, 7]. Maladaptation of the uterine vasculature that occurs during gestation is biologically and clinically significant as insufficient elevations of UBF are seen in pathological pregnancies (i.e. preeclampsia) [8, 9] which depending on the severity of the preeclampsia globally reduces levels of estrogens [10]. Insufficient UBF leads to diminished nutrient delivery, which is associated with fetal intrauterine growth restriction, higher prenatal and neonatal morbidity, and sometimes in severe cases leads to maternal and perinatal mortality, which are reported to occur in 6–14 per 1000 live births in the USA [7, 9, 11, 12].

In vivo ovine models have demonstrated that the increases in UBF are temporally associated with rises in the local and/or systemic endogenous estrogen levels during the follicular phase and normal pregnancy [2, 4, 7, 13–15]. Furthermore, reductions in local UBF were observed when unilateral intrauterine artery infusion of ICI 182780, a nonspecific estrogen receptor (ESR) antagonist, was performed in three chronically instrumented ovine models of endogenous and exogenous estrogen-induced increases in UBF [2]. Thus, in vivo models implicate ESRs in the regulation of UBF [2, 13]. We have previously reported the ex vivo relative change in ESR1 and ESR2 (ER-α and ER-β, respectively) protein expression levels in several reproductive and nonreproductive endothelia under different hormonal milieu (luteal, follicular, and pregnant physiologic states) [15, 16]. Compared to the luteal phase, ESR1 protein levels increased in the uterine (not systemic) artery endothelium during the follicular phase and pregnancy [15, 16], whereas ESR2 protein levels were higher in uterine, mammary, and placental endothelia only during pregnancy, thus inferring a broader role for ESR2-mediated pathways in all reproductive rather than systemic vasculature studied especially during gestation [15, 16].

Both ESR1 and ESR2 orchestrate rapid nongenomic and long-term genomic estrogenic effects on the endothelium [15, 17–20]. Rapid estrogen effects were observed to induce complex signaling mechanisms in numerous endothelial cell types and vascular beds [10, 15, 21–25]. Moreover, the very rapid uterine vasodilator responses to estrogen via ESR1 and/or ESR2 have to a great extent been attributed to be endothelial-mediated responses [24, 26–28]. These complex signaling mechanisms contributed to the increased nitric oxide (NO) production that leads to increases in UBF [23, 28–35]. In endothelial cells, ESRs are known to localize to different intracellular locations [28, 36–38], including potentially a small population to the plasma membrane which, in turn, serves to direct the rapid estrogenic responses, such as biosynthetic vasodilator responses, i.e. NO and prostacyclin (PGI_2) production [10, 39–41]. Moreover, studies by Acconcia et al. [42] clearly identified that the ESR1 requires palmitoylation as a post-translational modification to target the receptor to the plasma membrane of HeLa cells. Others have verified these findings in CHO cells [43] and in in vivo studies of ovarian and uterine responses to estrogen [44]. Our previous studies, using the pregnant uterine artery endothelial cells (P-UAECs) model that maintains a pregnancy-specific signaling and vasodilator phenotype, revealed the existence of membrane ESRs that increase NO with the membrane-impermeable estradiol-17β conjugate [39]. More recently, we demonstrated that ESR1 and ESR2 are both responsible for these rapid NO effects in UAECs independently of each other [41]. Membrane-bound ESR1 is known to co-localize to specialized, dynamic plasma membrane domains called caveolae. The caveolae compartmentalize many receptors and signaling molecules, including endothelial nitric oxide synthase (eNOS) [36, 38, 45–50]. Caveolae maintain their ʊ-shaped plasma membrane invagination via high levels of cholesterol and its main resident scaffolding protein, caveolin-1 (Cav-1) [38, 51–54]. In endothelium, the enzyme responsible for the de novo production of NO, eNOS, co-localizes with and is thought to be negatively regulated by Cav-1 [38, 46, 53, 55]. Several studies have been focused on understanding the protein–protein interaction between ESR1, Cav-1, and signaling molecules that ultimately activate eNOS located in the caveolae [36, 53, 55]. However, as compared to the extensive data for ESR1, less is known regarding ESR2 subcellular location to the plasma membrane caveolar structures, its interaction with Cav-1, or its mechanism to increase NO bioavailability. This is important based on our recent observations that both ESR1 and ESR2 very rapidly stimulate P-UAEC NO biosynthesis in culture [41]. Consistent with our recent data, Corcoran et al. [24] also showed that in ex vivo pre-contracted human myometrial arteries agonists to both ESR1 (PPT) and ESR2 (DNP) induce partial relaxation in an endothelial and NO-dependent manner.

Therefore, we hypothesize that ESR1 and ESR2 display similar spatial partitioning between the plasma membrane, the cytosol, and the nucleus and have similar interactions with Cav-1 protein at the plasma membrane in P-UAECs. The objectives of this study therefore were to (1) identify the location of ESR1, ESR2, and Cav-1 relative to specific regions of the plasma membrane in P-UAECs; (2) identify regions within ESR1 and ESR2 that can potentially interact with the plasma membrane by utilizing two bioinformatic prediction algorithms; and (3) identify the specific protein–protein interactions between Cav-1 with either ESR1 or ESR2 using both sucrose density centrifugation and a column-based immunoisolation technique in tandem with western blot analysis.

Materials and methods

Cell preparation and culture

The University of Wisconsin-Madison research animal care committees of the Medical School and the College of Agriculture and

Life Sciences approved all procedures and protocols for animal handling and experiments, which follow the recommended American Veterinary Medicine Association guidelines for humane treatment and euthanasia of laboratory farm animals. Uterine arteries were obtained from mixed Western breed pregnant ewes at 120–130 days' gestation during nonsurvival surgery as previously described [33, 56, 57]. Uterine arteries were dissected free of connective tissue, fat, and veins. Arteries were rinsed free of blood using medium 199 before tying off arterial branches, clamping off the larger diameter end, and inflating with medium 199 containing 5 mg/ml collagenase B (Roche Molecular Biochemicals) and 0.5% BSA through a three-way stop cock tap. Digestion was allowed to proceed at 37°C for 55 min before flushing the collagenase solution and endothelial cell sheets from the inner surface of the vessel and FACS sorted with Alexa 488 acetylated LDL (Invitrogen, L-23380). The isolated and validated UAECs were cultured in growth media HyClone Minimal Essential Medium with Earle's (MEM/EBSS) with 20% FBS, 100 mg/ml penicillin, and 100 mg/ml streptomycin and propagated [56]. For experiments, passage 3, P-UAECs were plated in T75 flasks containing phenol free endothelial basal medium (Lonza, Walkersville, MD) supplemented with 20% FBS and 1% penicillin-streptomycin.

Transmission electron microscopy and immunogold labeling

At passage 4 and ~90% confluence, endothelial cells were transferred to poly-L lysine cellware 12 mm round coverslips for preparation for transmission electron microscopy (TEM) and immunogold labeling [50, 58, 59]. Samples were sectioned parallel or perpendicular to the coverslip surface for TEM using a Reichert-Jung Ultracut-E Ultramicrotome and contrasted with Reynolds lead citrate and 8% uranyl acetate in 50% EtOH. Ultrathin sections were observed with a Philips CM120 electron microscope, and images were captured with a Mega View II side-mounted digital camera. See supplement for detailed methods of this technique.

Prediction of transmembrane domains within proteins

The *Ovis aries*-derived protein sequence for Caveolin-1 (Accession NP_001009477; 178aa), ER-α (Accession No. AAK52104; 431 amino acids), and ER-β (Accession No. NP_001009737; 527 amino acids), eNOS (Accession: NP_001123373; 1205aa—the accession number for the same database for all DNA sequences)—were input into the online Biology Workbench 3.2 database, http://workbench.sdsc.edu/. These software applications were used to predict ternary structures in the protein sequence studied. These sequences were input into the TMAP algorithm that uses Kyte-Doolittle hydropathy profile to identify hydrophobic residues that could potentially be membrane-spanning domains [60]. The sequences were also input into the TMHMM algorithm, which uses the Hidden Markov Model to predict transmembrane alpha helices or the location of an intervening loop region [61].

Protein extraction and western immunoblotting analysis

The total cell extracts were collected using a disposable cell scraper, vortexed, and clarified by centrifugation (13,000 × g, 5 min). The protein content of the samples was measured by a Bio-Rad procedure using BSA as the standard. Aliquots of the extracts were frozen at –80°C until western blot analysis could be performed. Equal amounts of total cell lysates were heated to denatured (95°C, 10 min) in Laemmli buffer, separated on precasted 4–20% SDS-PAGE, and electrically (100 V, 55 min) transferred to PVDF membranes [15, 16, 54, 56, 57]. Membranes were used to identify ER-α and ER-β detected using rabbit anti- ESR1 (HC-20; sc-543 [1:500]; Santa Cruz Biotechnology Inc.), rabbit anti-ESR2 (H-150; sc-8974 [1:500]; Santa Cruz Biotechnology Inc), and rabbit anti-Cav-1 (No. 3238 [1:10,000]; Cell Signaling Technology). The corresponding secondary antibody was used at a dilution factor of 1:1000 (ESR1 and ESR2), 1:10,000 (Cav-1), and anti-β-actin dilution factor of 1:3000. In addition, cell fractionation studies also included the verification of correct fractionation by utilizing western immunoblotting analysis using Plasma Membrane Fraction Western Blot Cocktail (Abcam—ab139413). Anti-mouse secondary antibody was used as 1:1500 dilution. These particular ESR1 and ESR2 antibodies and dilutions were chosen since they showed optimal data that were very consistent with our numerous previous ESR1 and ESR2 studies [15, 16, 40, 57].

Subcellular protein fractionation

Fractionation was achieved by using the Subcellular Protein Fraction Kit for Cultured Cells (Thermo Scientific No. 78840). The manufacturer's protocol was followed and the samples analyzed using western immunoblotting with the ESR1 and ESR2 antibodies described above. Purity of the fraction was validated for plasma membrane (Na^+/K^+ATPase), cytosol (GAPDH), and Chromatin (Histone H3) using antibodies to standard markers.

Caveolae isolation

Caveolae isolation was performed as described previously [50, 54, 62]. Briefly, passage 3 P-UAECs were grown to approximately 90% confluence in a T75 flask and then split (passage 4) into 10 T75s for each cell line; five T75s were used as control the others for estrogen treatment. Following treatment, for each cell line, cells were collected in 0.5 mL sodium carbonate buffer (pH = 11) containing phosphatase and protease inhibitors. The proteins from the respective five T75s were pooled and then caveolar isolation was performed using discontinuous sucrose density gradient centrifugation. A light scattering band confined to the 5–35% sucrose interface was enriched with caveolar membranes. Fifteen 1-ml fractions were collected and analyzed using western immunobloting for ESR1, ESR2, and Cav-1 proteins.

Immunoisolation Cav-1 columns

P-UAEC lysates were loaded with beads (Carbolink Immobilization kit, Pierce, Rockford, IL) covalently coupled to customed ordered anti-cav-1 antibody (Cell Signaling Tech. Inc.). The cav-1 bound fraction was subsequently eluted according to the manufacturer's instructions and this fraction was analyzed using western immunoblotting and scanning densitometry, as previously performed and described [54]. Indeed, the same protein elulates used in this previous study were utilized in the current study. See supplement for detailed methods of this technique.

Materials

Electron Microscope: FEI, Tecnai T-12

Antibody Name	Lot number	References	RRID
ESR1	sc-543	PMID:28028198, PMID:28323976, PMID:28475868, PMID:28938408	AB_631471
ESR2	sc-8974	PMID:28962900	AB_2102246
Caveolin-1	3238	PMID:28017794,	AB_2072166

Statistical analysis

Data are representative of n = 3 or n = 4 separate experiments and presented as means ± SEM. P-UAECs each isolated from different experimental animals. ANOVA followed by the Bonferroni multiple comparison test was performed as post hoc analysis or Student's *t*-test was used to determine differences between treatments and controls. Significant was established a priori at $P < 0.05$. Statistical analyses were performed with GraphPad Prism 5.0b software.

Results

Transmission electron microscopy and immunogold labeling

We first identified the location of the classic ʊ-shaped caveolae invaginations using TEM. We observed numerous caveolae near and at the plasma membrane of P-UAECs. These invaginations were identified in regions near cell-cell attachments (Figure 1A) and the leading edge of the endothelial cell (Figure 1B). TEM and immunogold labeling, depicted as black dots, identified the intracellular location for ESR1 and Cav-1 in P-UAECs (Figure 2). Figure 2A insert illustrates the IgG control sample showing no immunogold staining. ESR1 was found to localize at the plasma membrane, the cytosol, and nucleus (Figure 2B). The antibody for ESR2 did not work for this immunogold staining procedure (not shown). As expected, Cav-1 localized strictly to punctate regions of the plasma membrane without showing the distinct hourglassstructure of caveolae that are altered during the harsh fixation process (Figure 2C).

Subcellular protein fractionation

In order to further interrogate cellular localization of the ESRs in UAECs, we also performed subcellular fractionation experiments. Whole cell P-UAEC lysates and brain tissue were used as positive controls. Western immunoblot analyses of ESR1 (Figure 3A) and ESR2 (Figure 3B) proteins were identified within the membranes, cytoplasmic, nuclear, and cytoskeletal fractions. Under these unstimulated conditions, chromatin ESR2, but not ESR1, immunostaining was detected. Although only one antibody each was used in our demonstration of ESR2, but not ESR1, chromatin interaction, this finding is in keeping with the observations that under nonstimulation condition, ESR2 readily interacts with chromatin possibly even without ligand binding. However, the current data do not exclude ESR1 interaction with chromatin under estrogen stimulation [63].

Prediction of transmembrane domains within protein

We then utilized two bioinformatic prediction algorithms, TMAP (Supplementary Figure S1) and TMHMM (Figure 4), to identify regions within ESR1 and ESR2 that can potentially facilitate attachment at the plasma membrane [60, 61]. Analysis of ESR1protein sequence with the TMAP algorithm identified two segments of approximately 20 amino acids (aa). These segments were recognized as regions for ligand binding [62] and co-activator recognition sites [64] (Supplementary Figure S1A). In analyzing ESR2 protein sequence, the TMAP algorithm identified one segment of approximately 15 aa within the protein. This 15 aa segment was recognized as a region for ligand binding and the co-activator recognition site [64] (Supplementary Figure S1B). The analyses of Cav-1 and eNOS using this algorithm predicted sites that could potentially interact with the plasma membrane (data not shown). In the analyses of ESR1 and ESR2 protein sequences using TMHMM, there was zero probability that these proteins would respectively have an alpha helix structure or a location for an intervening loop region that could interact with the plasma membrane (Figure 4A and B). When the Cav-1

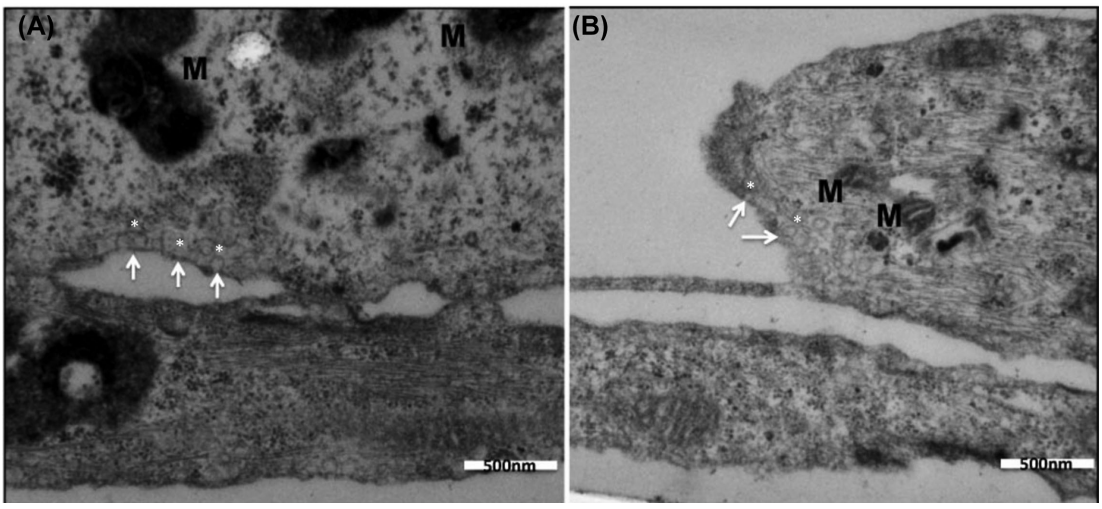

Figure 1. Transmission electron micrograph (TEM) identifying distinct caveolae structures in the uterine artery endothelial cell (UAEC) plasma membrane. The caveolae were found to line up along the length of the plama membrane, (A) the regions close to cell–cell contacts, and (B) the leading edge of the cell. The darker intracellular discs are mitochondria. Arrows point to the ʊ-shaped caveolae invaginations. M = mitochondria.

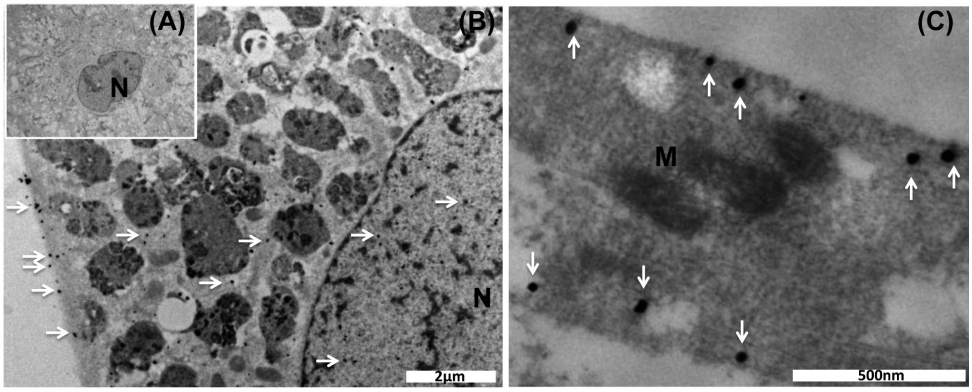

Figure 2. Transmission electron micrograph (TEM) identifying immunogold labeled ESR1 and caveolin-1 proteins in the uterine artery endothelial cells derived from the pregnant state (P-UAEC). (A) IgG control samples were incubated with IgG antibody followed by secondary antibody containing immunogold particles. (B) Immunogold labeling of ESR1 identified the protein localization at the plasma membrane, the cytosol, and the nucleus. (C) Illustrates the location of Cav-1 close to or at the plasma membrane. Immunogold labels are identified by small black dots. M = mitochondria, N = nucleus.

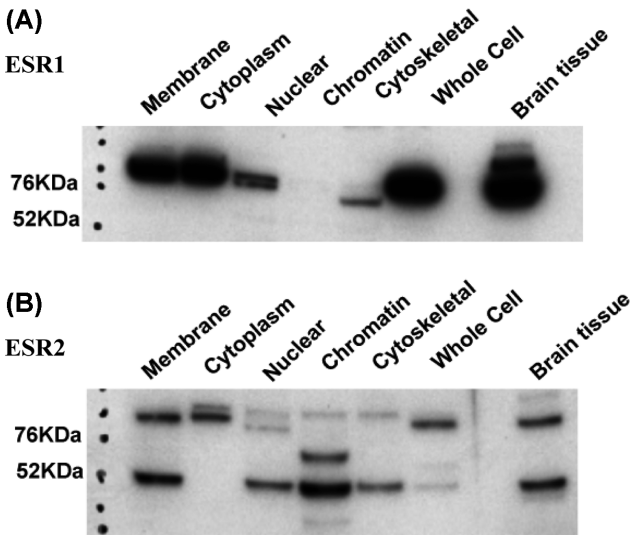

Figure 3. Subcellular fractionation to identify the location of ESR1 and ESR2 in uterine artery endothelial cells derived from the pregnant state (P-UAEC). Whole cell lysates were used for subcellular protein fractionation kits for cultured cells (Thermo Scientific) to identify the location of ESR1 and ESR2 in P-UAECs. The fractionations collected were analyzed using western immunoblotting and probed with ESR1 or ESR2 antibodies. (A) ESR1 was detected in the membrane, cytosolic, and at lower levels in the nuclear and cytoskeletal fractions. (B) ESR2 was detected in the membrane, cytosolic, nuclear, chromatin, and cytoskeletal fractions as both a monomer (~55 KDa) and dimer (110 KDa). Whole cell lysates from P-UAECs and brain tissue were used as positive controls. Fractions were defined based on standard markers of plasma membrane (Na^+/K^+ATPase), cytosol (GAPDH), and chromatin (Histone H3) markers.

protein sequence was analyzed using TMHMM, a region between amino acids 95–120 demonstrated a 100% probability of being a transmembrane segment (Figure 4C).

Caveolar isolation

Next we performed sucrose density centrifugation to evaluate if ESR1 and ESR2 are present in caveolae-enriched preparations. In these studies, we combined P-UAECs fractions 4–7 that were identified as Cav-1 highly enriched [54] and observed ESR1 localized to both the caveolar and as expected the noncaveolar (lanes 9–12) fractions (Figure 5). By contrast, ESR2 was completely undetectable using this antibody within the caveolae fraction, but on the same western blots, ESR2 was strongly detected in the noncaveolar fractions thus also serving as a positive control for the antibody used. Fraction 8 was omitted in the ESR analysis based on Cav-1 immunostaining to clearly differentiate the difference between caveolae and noncaveolae fractions relative to fraction markers.

Immunoisolation Cav-1 columns

To directly evaluate the protein–protein interactions between Cav-1 and either ESR1 or ESR2 and relative to their location within the caveolae, we developed a column-based immunoisolation method using Cav-1 antibody [54]. These studies were also performed to confirm and validate our observations using sucrose density centrifugation. In Figure 6, we evaluated the relative levels of ESR1 and ESR2 in Cav-1 bound eluates from the immunoisolation columns. Cav-1 and ESR1 protein–protein interactions were clearly detected in the Cav-1 bound fraction whereas ESR2 did not bind to Cav-1 demonstrating a complete absence of physical association between ESR2 and Cav-1 thus validating and confirming those data presented above in Figure 5.

Discussion

In the current study, we evaluated in P-UAECs the spatial partitioning of ESR1 and ESR2 between the plasma membrane, the cytosol, and the nucleus of UAECs and then directly determined for the first time the differential protein–protein interactions of both ESR1 and ESR2 with Cav-1 protein. The major observations we report herein are as follows: (1) the caveolar structures at the P-UAEC plasma membrane, ESR1, and ESR2 were identified to be present in several subcellular locations including the plasma membranes where their estrogenic effects influence rapid endothelial biological functions; (2) the bioinformatic predictions identified that neither ESR1 nor ESR2 contains a transmembrane region that can cross the plasma membrane; and (3) we were able to identify in caveolae a physical direct association between Cav-1 and ESR1 and contrary to our hypothesis, the complete lack of association between Cav-1 and ESR2, therefore identifying for the first time a novel difference of ESR regulation in P-UAECs. In addition to the difference in association between Cav-1 and the ESRs, we were also able to detect ESR1,

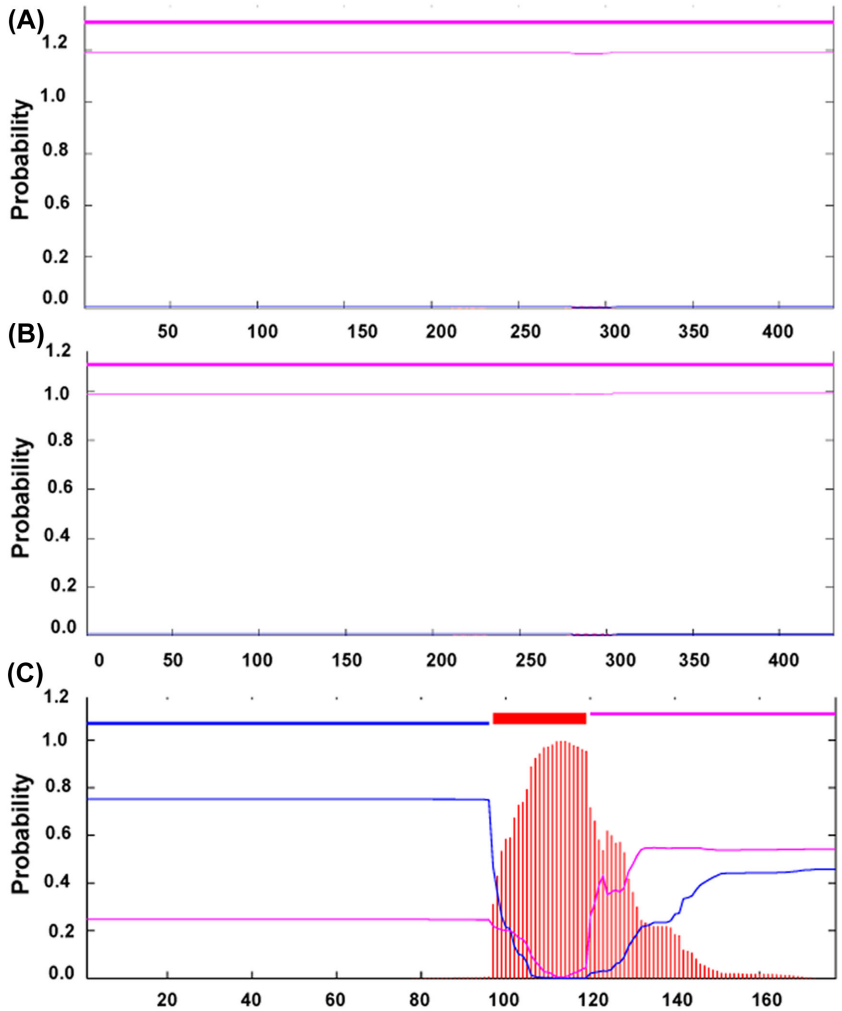

Figure 4. The TMHMM algorithm profile for ESR1, ESR2, and Cav-1. TMHMM algorithm provides a probability index for alpha helix or intervening loop regions within a protein sequence and TMHMM revealed that neither (A) ESR1 nor (B) ESR2 contain segment(s) resembling an alpha helix or intervening loop region that may potentially interact and/or anchor the protein within the plasma membrane. (C) The TMHMM algorithm also reveals that Cav-1 contains a segment, with high probability, to contain an alpha helix or intervening loop that can interact with plasma membrane.

but not ESR2, within the caveolae microdomains, supporting the protein–protein interaction observed between Cav-1 and ESR1.

In the present study, we sought to identify caveolae structures and the location of ESR1 and ESR2 within P-UAECs and the caveolae. The understanding of the ESRs in the caveolae is significant due to the different rapid nongenomic membrane versus prolonged genomic (nuclear) estrogenic effects on the endothelium. We first used TEM in order to identify caveolar structures within the plasma membrane of UAECs and to for the first time more precisely used immunogold techniques localize ESR1 and ESR2 to the plasma membrane, cytoplasm, and nucleus. The former data are consistent with several others that observed the caveolae structures localize at the plasma membrane of numerous endothelial cells types and that these structures assume the classic ʊ-shaped invaginations [47, 50, 65, 66]. We theorized that respective location of ESR1 and ESR2 would be important for understanding the rapid NO-mediated uterine vasodilatory effects on the endothelium by estrogen that we previously reported in vivo [2, 5, 13, 29, 67, 68] and in vitro [24, 39, 41, 69, 70]. In the present study, ESR1 was detected in the plasma membrane as well as several intracellular locations similar to other reports that studied the cardiovascular system especially the endothelium and numerous endothelial cell types [40, 47, 65, 71]. We further verified this for the first time using both immunogold labeling and subcellular protein fractionation. Unlike ESR1, the visual identification of ESR2 location using immunogold labeling was unsuccessful due to either the apparent lack of specificity in the available antibodies or the difficulty for these antibodies to access the epitope of the relatively intact protein in a cell. In contrast, our subcellular fractionation data clearly showed that ESR2 is indeed present within the membrane, cytosol, and nuclear fractions, as seen in previously reports [72, 73], none of which tried to explicitly define a caveolar localization of ESR2. Unfortunately, the harsher chemical sample processing required for immunogold labeling of our proteins did not allow for a clear identification of the caveolae structures along with co-localization with ESR1 or ESR2 with gold particles.

Therefore, to further assess the potential localization of ESR1 and ESR2 to the plasma membrane, we utilized for the first time bioinformatic predictions to identify potential transmembrane regions that could facilitate anchoring of ESR1, ESR2, and/or Cav-1 to the endothelial plasma membrane. The two algorithms that we

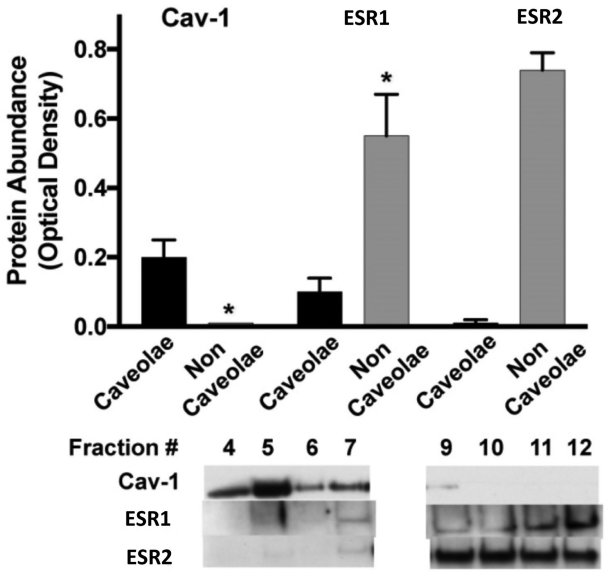

Figure 5. ESR1 and ESR2 locations within the caveolae in uterine artery endothelial cells derived from the pregnant state (P-UAECs). Caveolae isolation was achieved using whole cell lysates loaded on a sucrose density gradient solution. Immunoblot analysis of caveolae fractions (top row) was defined by cav-1 protein enrichment (lanes 4–7) and noncaveolae fractions devoid of cav-1 (lines 9–12). Fraction 8 was not use for analysis. ESR1 was detected in both caveolae and noncaveolae fractions (middle row), whereas ESR2 was only detected in the noncaveolae fractions (bottom row). $^{*}P > 0.05$.

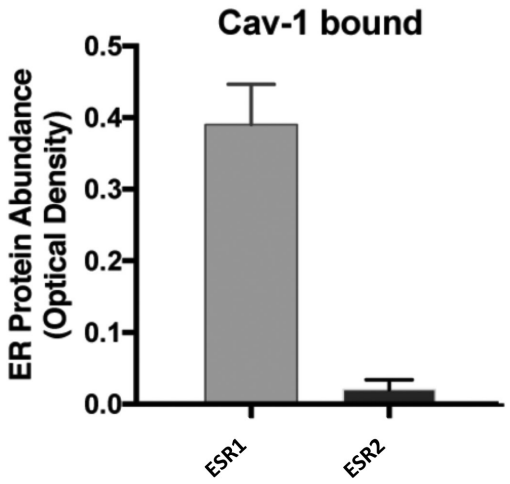

Figure 6. ESR1 and ESR2 protein–protein interaction with Cav-1 in uterine artery endothelial cells derived from the pregnant state (P-UAECs). Whole cell lysate were loaded onto beads (Carbolink Immobilization kit) that were coupled to anti-cav-1 antibody for immunoisolation in order identify protein–protein interactions between Cav-1 and ESR1 or ESR2 and analyzed using western immunoblot analysis. Protein–protein interactions between Cav-1 and ESR1, but not ESR2, were observed; the latter indicating that these proteins do not interact.

employed identified no transmembrane regions within either ESR1 or ESR2 that would allow these receptors to be inserted into the plasma membrane [60, 61]. Although TMHMM showed zero probability of the ESRs has an alpha helix structure or a location for an intervening loop region that can interact with the plasma membrane, these findings further validate the use of these algorithms in predicting these types of regions from the protein sequence. However, the lack of these candidate regions within the ESRs secondary structures does not preclude other cellular mechanisms such as post-translational modification from facilitating their targeting to and in close interaction with the membrane. For example, acylation (i.e. N-myristoylation or palmitoylation) is a known post-translational modification that is well documented to be key for eNOS being targeted to the caveolae [74, 75]. TMAP and TMHMM identified a specific region within Cav-1 protein sequence that would allow a direct interaction between the protein and the membrane; this observation is consistent with our current TEM and Cav-1 immunogold data (Figure 1). Cav-1 is also acylated in order to facilitate its interaction with the plasma membrane in addition to the hydrophobic region we were able to identify in this study (Figure 4C). The identified hydrophobic region within Cav-1 protein sequence allows for a direct interaction with the membrane; this observation is consistent with conclusions of other studies that Cav-1 maintains the classical ʊ-shaped invaginations at the membrane [66, 76].

Estrogenic effects are known to occur acutely or chronically (nongenomic and genomic); therefore, the regulatory mechanisms that govern these effects are likely dependent on several significant protein–protein interactions [15, 51]. One important known level of regulation may involve the acute interaction between ESR1 and/or ESR2 with Cav-1 [15, 38, 63, 72, 77]. The current sucrose density caveolae isolation demonstrated ESR1 detection within the caveolae fractions. In the current study, we also report for the first time that ESR1 column-based immunoisolates with Cav-1 antibody [54] demonstrated a very close protein–protein association of these proteins in UAECs. Cav-1 and ESR1 interactions also directly suggest that Cav-1 may help translocate ESR1 to the plasma membrane where it is assembled with other signaling molecules within the caveolae [38, 54]. As we and others have previously described, the caveolae are known to concentrate a plethora of receptors and signaling transducing kinases that rapidly facilitate the response to stimuli that is received by the endothelium [15, 38, 48, 49, 51, 54, 78]. Using sucrose density centrifugation, we present the novel observation that indeed ESR1, but not ESR2, was localized to the caveolar-enriched fractions, whereas as expected both receptors subtypes were present at high levels in the noncaveolar fractions. However, herein we also validated this and report for the first time that there was little to no protein–protein interaction observed between ESR2 and Cav-1. Thus, these data are the first to demonstrate that plasma membrane ESR2, unlike ESR1, is not localized to the caveolae. Pedram et al. [43] reported an elegant study in which they discovered a signature 9 amino acid motif suggesting it as a unifying mechanism for sex steroid receptors to translocate to the plasma membrane. They also directly proved that palmitoylation increases the physical association of ESR1 with the plasma membrane and facilitates Cav-1 association using siRNA for Cav-1 in transfected CHO cells. Their ESR1 Cav-1 conclusions are consistent with many other studies including the current data presented in Figures 5 and 6 [65, 79, 80]. They made similar assumptions for the ESR2; however, they did not show data on IP of ESR2 identifying Cav-1 co-IP using CHO cells and thus did not directly prove localization to the same plasma membrane location by interacting with Cav-1. Our current novel data directly demonstrate that ESR2 utilizes a Cav-1-independent localization in the endothelial plasma membrane which we propose explain some of the differences observed between rapid estrogenic actions of ESR2 versus those of ESR1 in increasing bioavailability of vasodilators, i.e. NO [41] and PGI_2 [10]. Particularly given that our recently reported data demonstrating that activation of

either ESR1 or ESR2 increases NO biosynthesis [41], whereas PGI_2 increased in an ESR1-dependent manner with no ESR2 involvement in P-UAECs [10]. Taken together, these novel data suggest that increased NO bioavailability is driven in a Cav-1-dependent and independent mechanism (ESR1 and ESR2, respectively) while PGI_2 is only regulated via a Cav-1-dependent ESR1 pathway. In future studies, altering the raft compartment to disrupt ESR1 and/or ESR2 association by depleting cholesterol or Cav-1 and determining the effects on NO versus PGI_2 production responses to estrogen treatments will provide functional clues of the individual contributions of these two ESR subtypes relative to caveolae. In addition, in human umbilical vein endothelial cells, a widely used endothelial cell model, only the combined treatment of ESR1and ESR2-specific agonists was required to mimic the rapid estradiol-17β-induced S-nitrosylation of proteins [63]. However, the role of Cav-1 in protein S-nitrosylation or the signaling pathway activated by the ESRs is unknown.

Perspectives and significance

Estrogen and its receptors, ESR1 and ESR2, are important contributors in women's cardiovascular health and especially in the reproductive vascular beds (e.g. uterine, ovarian, and mammary). These receptors exert rapid short-term and slow long-term effects on the vasculature and have an important role in uterine vascular adaptations during pregnancy. Our work with P-UAECs identified abundant caveolae structures and the ESRs intracellular locations. We also identified for the first time a key difference in protein–protein interactions between the ESR1 and ESR2 with Cav-1. The closer interaction between ESR1 and Cav-1 points to estrogen/ESR1 rapid effect that is Cav-1 dependent, whereas we report for the first time that ESR2 appears to be regulated at the plasma membrane in a Cav-1-independent manner. Therefore, we identified a novel distinctive interaction between ESR1 and ESR2 with Cav-1, highlighting a potential differential regulatory mechanism in the rapid estrogenic effects in P-UAECs. Delineating mechanisms establishing the role of estrogen and ESRs in the uterine endothelial vasodilatory phenotype of pregnancy provides greater understanding of specific mechanisms functioning abnormally in gestational vascular pathophysiology such as hypertension and preeclampsia. Exploiting such differences in previously unrealized regulatory role of Cav-1 over ESR-mediated signaling may point to a potential therapeutic target to alleviate cardiovascular dysfunction in gestational diseases such as preeclampsia.

Supplementary data

Supplementary data are available at *BIOLRE* online.

Supplement Figure 1. The TMAP algorithm profile for ESR1 and ESR2. TMAP algorithm uses Kyte-Doolittle Hydrophaphy Profile to identify hydrophobic regions. This algorithm analyzed 15aa (solid line) or 4aa (dashed line) to quantify the hydrophobicy within a given sequence. (A) TMAP revealed that ESR1 contains two segment containing highly hydrophobic residues as identified by the solid bar on the top of the graph. These regions are part of the ligand-binding and co-activator binding sites. (B) The TMAP algorithm also reveals that ESR2 contains a segment with highly hydrophobic residues, which also align with the ligand-binding domain. Both Cav-1 and eNOS show no 15aa or 4aa segments with high level of hydrophobicity (data not shown).

Acknowledgments

We wish to thank, Chi Zhou, Ph.D., Bryan C. Ampey, Ph.D., Gladys E. Lopez, M.S., Cindy L. Goss, Terrance M. Phernetton, Jason L. Austin, and Ravi Balijepalli, Ph.D. at the University of Wisconsin-Madison. We also wish to thank Vladimir E. Vargas, Ph.D., A. Umit Kayisli, Ph.D., Maja Okuka, and Jessica S. Youngblood at the University of South Florida.

References

1. Rosenfeld CR. Distribution of cardiac output in ovine pregnancy. *Am J Physiol* 1977; **232**:H231–H235.
2. Magness RR, Phernetton TM, Gibson TC, Chen DB. Uterine blood flow responses to ICI 182 780 in ovariectomized oestradiol-17beta-treated, intact follicular and pregnant sheep. *J Physiol* 2005; **565**(1): 71–83.
3. Reynolds LP, Redmer DA. Utero-placental vascular development and placental function. *J Anim Sci* 1995; **73**(6):1839–1851.
4. Magness RR. Maternal cardiovascular and other physiological response to the endocrinology of pregnancy. In: Bazer FW, ed. The endocrinology of pregnancy. Totowa, NJ: Human Press Inc.; 1998: 507–539.
5. Magness RR, Phernetton TM, Zheng J. Systemic and uterine blood flow distribution during prolonged infusion of 17beta-estradiol. *Am J Physiol* 1998; **275**:H731–H743.
6. Magness RR, Ford SP. Maternal cardiovascular adaptation and uterine circulation-physiology and pathophysiology. In: *Stress and Developmental Programming of Health and Disease: Beyond Phenomenology*. Hauppauge, NY: Nova Science Publishers, Inc. 2014; Chapter 7:341–374.
7. Magness RR, Zheng J. Maternal Cardiovascular Alterations During Pregnancy. *In: Pediatrics and Perinatology: The Scientific Basis. 2nd edition, Editors: Gluckman, P.D., and Heymann, M.A., Arnold Publishing, London*. 1996: pp. 762–772.
8. Sladek SM, Magness RR, Conrad KP. Nitric oxide and pregnancy. *Am J Physiol* 1997; **272**:R441–R463.
9. Zamudio S. High-altitude hypoxia and preeclampsia. *Front Biosci* 2007; **12**(8-12):2967–2977.
10. Jobe SO, Ramadoss J, Wargin AJ, Magness RR. Estradiol-17beta and its cytochrome P450- and catechol-O-methyltransferase-derived metabolites selectively stimulate production of prostacyclin in uterine artery endothelial cells: role of estrogen receptor-alpha versus estrogen receptor-beta. *Hypertension* 2013; **61**(2):509–518.
11. Carbillon L, Uzan M, Uzan S. Pregnancy, vascular tone, and maternal hemodynamics: a crucial adaptation. *Obstet Gynecol Surv* 2000; **55**(9):574–581.
12. Kramer MS. The epidemiology of adverse pregnancy outcomes: an overview. *J Nutr* 2003; **133**(5):1592S–1596S.
13. Gibson TC, Phernetton TM, Wiltbank MC, Magness RR. Development and use of an ovarian synchronization model to study the effects of endogenous estrogen and nitric oxide on uterine blood flow during ovarian cycles in sheep. *Biol Reprod* 2004; **70**(6):1886–1894.
14. Sprague BJ, Phernetton TM, Magness RR, Chesler NC. The effects of the ovarian cycle and pregnancy on uterine vascular impedance and uterine artery mechanics. *Eur J Obstet Gynecol Reprod Biol* 2009; **144**(Suppl 1):S170–S178.
15. Pastore MB, Jobe SO, Ramadoss J, Magness RR. Estrogen receptor-alpha and estrogen receptor-beta in the uterine vascular endothelium during pregnancy: functional implications for regulating uterine blood flow. *Semin Reprod Med* 2012; **30**(1):46–61.
16. Byers MJ, Zangl A, Phernetton TM, Lopez G, Chen DB, Magness RR. Endothelial vasodilator production by ovine uterine and systemic arteries: ovarian steroid and pregnancy control of ERalpha and ERbeta levels. *J Physiol* 2005; **565**(1):85–99.
17. Bilsel AS, Moini H, Tetik E, Aksungar F, Kaynak B, Ozer A. 17beta-Estradiol modulates endothelin-1 expression and release in human endothelial cells. *Cardiovasc Res* 2000; **46**(3):579–584.

18. Wang L, Andersson S, Warner M, Gustafsson JA. Estrogen receptor (ER)beta knockout mice reveal a role for ERbeta in migration of cortical neurons in the developing brain. *Proc Natl Acad Sci USA* 2003; **100**(2):703–708.
19. Hishikawa K, Nakaki T, Marumo T, Suzuki H, Kato R, Saruta T. Up-regulation of nitric oxide synthase by estradiol in human aorticendothelial cells. *FEBS Lett* 1995; **360**(3):291–293.
20. Chakrabarti S, Morton JS, Davidge ST. Mechanisms of estrogen effects on the endothelium: an overview. *Can J Cardiol* 2014; **30**(7):705–712.
21. Haynes MP, Sinha D, Russell KS, Collinge M, Fulton D, Morales-Ruiz M, Sessa WC, Bender JR. Membrane estrogen receptor engagement activates endothelial nitric oxide synthase via the PI3-kinase-Akt pathway in human endothelial cells. *Circ Res* 2000; **87**(8):677–682.
22. Russell KS, Haynes MP, Caulin-Glaser T, Rosneck J, Sessa WC, Bender JR. Estrogen stimulates heat shock protein 90 binding to endothelial nitric oxide synthase in human vascular endothelial cells. *J Biol Chem* 2000; **275**(7):5026–5030.
23. Stefano GB, Prevot V, Beauvillain JC, Cadet P, Fimiani C, Welters I, Fricchione GL, Breton C, Lassalle P, Salzet M, Bilfinger TV. Cell-surface estrogen receptors mediate calcium-dependent nitric oxide release in human endothelia. *Circulation* 2000; **101**(13):1594–1597.
24. Corcoran JJ, Nicholson C, Sweeney M, Charnock JC, Robson SC, Westwood M, Taggart MJ. Human uterine and placental arteries exhibit tissue-specific acute responses to 17beta-estradiol and estrogen-receptor-specific agonists. *Mol Hum Reprod* 2014; **20**(5):433–441.
25. Wyckoff MH, Chambliss KL, Mineo C, Yuhanna IS, Mendelsohn ME, Mumby SM, Shaul PW. Plasma membrane estrogen receptors are coupled to endothelial nitric-oxide synthase through Galpha(i). *J Biol Chem* 2001; **276**(29):27071–27076.
26. Shaw L, Taggart MJ, Austin C. Mechanisms of 17 β-oestradiol induced vasodilatation in isolated pressurized rat small arteries. *Br J Pharmacol* 2000; **129**(3):555–565.
27. Hisamoto K, Bender JR. Vascular cell signaling by membrane estrogen receptors. *Steroids* 2005; **70**(5-7):382–387.
28. Wu Q, Chambliss K, Umetani M, Mineo C, Shaul PW. Non-nuclear estrogen receptor signaling in the endothelium. *J Biol Chem* 2011; **286**(17):14737–14743.
29. Rosenfeld CR, Cox BE, Roy T, Magness RR. Nitric oxide contributes to estrogen-induced vasodilation of the ovine uterine circulation. *J Clin Invest* 1996; **98**(9):2158–2166.
30. Chambliss KL, Shaul PW. Estrogen modulation of endothelial nitric oxide synthase. *Endocr Rev* 2002; **23**(5):665–686.
31. Florian M, Lu Y, Angle M, Magder S. Estrogen induced changes in Akt-dependent activation of endothelial nitric oxide synthase and vasodilation. *Steroids* 2004; **69**(10):637–645.
32. Feldman RD, Gros R. Unraveling the mechanisms underlying the rapid vascular effects of steroids: sorting out the receptors and the pathways. *Br J Pharmacol* 2011; **163**(6):1163–1169.
33. Magness RR, Shaw CE, Phernetton TM, Zheng J, Bird IM. Endothelial vasodilator production by uterine and systemic arteries. II. Pregnancy effects on NO synthase expression. *Am J Physiol* 1997; **272**:H1730–H1740.
34. Magness RR, Sullivan JA, Li Y, Phernetton TM, Bird IM. Endothelial vasodilator production by uterine and systemic arteries. VI. Ovarian and pregnancy effects on eNOS and NO(x). *Am J Physiol Heart Circ Physiol* 2001; **280**(4):H1692–H1698.
35. Vonnahme KA, Wilson ME, Li Y, Rupnow HL, Phernetton TM, Ford SP, Magness RR. Circulating levels of nitric oxide and vascular endothelial growth factor throughout ovine pregnancy. *J Physiol* 2005; **565**(1):101–109.
36. Chambliss KL, Shaul PW. Rapid activation of endothelial NO synthase by estrogen: evidence for a steroid receptor fast-action complex (SRFC) in caveolae. *Steroids* 2002; **67**(6):413–419.
37. Fu XD, Cui YH, Lin GP, Wang TH. Non-genomic effects of 17beta-estradiol in activation of the ERK1/ERK2 pathway induces cell proliferation through upregulation of cyclin D1 expression in bovine artery endothelial cells. *Gynecol Endocrinol* 2007; **23**(3): 131–137.
38. Ramadoss J, Pastore MB, Magness RR. Endothelial caveolar subcellular domain regulation of endothelial nitric oxide synthase. *Clin Exp Pharmacol Physiol* 2013; **40**(11):753–764.
39. Chen DB, Bird IM, Zheng J, Magness RR. Membrane estrogen receptor-dependent extracellular signal-regulated kinase pathway mediates acute activation of endothelial nitric oxide synthase by estrogen in uterine artery endothelial cells. *Endocrinology* 2004; **145**(1):113–125.
40. Liao WX, Magness RR, Chen DB. Expression of estrogen receptors-alpha and -beta in the pregnant ovine uterine artery endothelial cells in vivo and in vitro. *Biol Reprod* 2005; **72**(3):530–537.
41. Pastore MB, Talwar S, Conley MR, Magness RR. Identification of differential ER-Alpha versus ER-Beta mediated activation of eNOS in ovine uterine artery endothelial cells. *Biol Reprod* 2016; **94**(6):139.
42. Acconcia F, Ascenzi P, Bocedi A, Spisni E, Tomasi V, Trentalance A, Visca P, Marino M. Palmitoylation-dependent estrogen receptor alpha membrane localization: regulation by 17beta-estradiol. *Mol Biol Cell* 2005; **16**(1):231–237.
43. Pedram A, Razandi M, Sainson RC, Kim JK, Hughes CC, Levin ER. A conserved mechanism for steroid receptor translocation to the plasma membrane. *J Biol Chem* 2007; **282**(31):22278–22288.
44. Adlanmerini M, Solinhac R, Abot A, Fabre A, Raymond-Letron I, Guihot AL, Boudou F, Sautier L, Vessieres E, Kim SH, Liere P, Fontaine C et al. Mutation of the palmitoylation site of estrogen receptor alpha in vivo reveals tissue-specific roles for membrane versus nuclear actions. *Proc Natl Acad Sci USA* 2014; **111**(2):E283–E290.
45. Liu J, Oh P, Horner T, Rogers RA, Schnitzer JE. Organized endothelial cell surface signal transduction in caveolae distinct from glycosylphosphatidylinositol-anchored protein microdomains. *J Biol Chem* 1997; **272**(11):7211–7222.
46. Couet J, Li S, Okamoto T, Ikezu T, Lisanti MP. Identification of peptide and protein ligands for the Caveolin-scaffolding domain. *J Biol Chem* 1997; **272**(10):6525–6533.
47. Frank PG, Woodman SE, Park DS, Lisanti MP. Caveolin, caveolae, and endothelial cell function. *Arterioscler Thromb Vasc Biol* 2003; **23**(7):1161–1168.
48. Feng L, Zhang HH, Wang W, Zheng J, Chen DB. Compartmentalizing proximal FGFR1 signaling in ovine placental artery endothelial cell caveolae. *Biol Reprod.* 2012; **87**(2):40, 1–9.
49. Feng L, Liao WX, Luo Q, Zhang HH, Wang W, Zheng J, Chen DB. Caveolin-1 orchestrates fibroblast growth factor 2 signaling control of angiogenesis in placental artery endothelial cell caveolae. *J Cell Physiol* 2012; **227**:2480–2491.
50. Liao WX, Feng L, Zhang H, Zheng J, Moore TR, Chen DB. Compartmentalizing VEGF-Induced ERK2/1 signaling in placental artery endothelial cell caveolae: a paradoxical role of caveolin-1 in placental angiogenesis in vitro. *Mol Endocrinol* 2009; **23**:1428–1444.
51. Shaul PW. Regulation of endothelial nitric oxide synthase: location, location, location. *Annu Rev Physiol* 2002; **64**:749–774.
52. Sargiacomo M, Sudol M, Tang Z, Lisanti MP. Signal transducing molecules and glycosyl-phosphatidylinositol-linked proteins form a caveolin-rich insoluble complex in MDCK cells. *J Cell Biol* 1993; **122**:789–807.
53. Feron O, Saldana F, Michel JB, Michel T. The endothelial nitric-oxide synthase-caveolin regulatory cycle. *J Biol Chem* 1998; **273**:3125–3128.
54. Ramadoss J, Liao WX, Morschauser TJ, Lopez GE, Patankar MS, Chen DB, Magness RR. Endothelial caveolar hub regulation of adenosine triphosphate-induced endothelial nitric oxide synthase subcellular partitioning and domain-specific phosphorylation. *Hypertension* 2012; **59**:1052–1059.
55. Grayson TH, Chadha PS, Bertrand PP, Chen H, Morris MJ, Senadheera S, Murphy TV, Sandow SL. Increased caveolae density and caveolin-1 expression accompany impaired NO-mediated vasorelaxation in diet-induced obesity. *Histochem Cell Biol* 2013; **139**:309–321.
56. Bird IM, Sullivan JA, Di T, Cale JM, Zhang L, Zheng J, Magness RR. Pregnancy-Dependent changes in cell signaling underlie changes in differential control of vasodilator production in uterine artery endothelial cells. *Endocrinology* 2000; **141**:1107–1117.

57. Jobe SO, Ramadoss J, Koch JM, Jiang Y, Zheng J, Magness RR. Estradiol-17beta and its cytochrome P450- and catechol-O-methyltransferase-derived metabolites stimulate proliferation in uterine artery endothelial cells: role of estrogen receptor-alpha versus estrogen receptor-beta. *Hypertension* 2010; **55**:1005–1011.
58. Markandeya YS, Fahey JM, Pluteanu F, Cribbs LL, Balijepalli RC. Caveolin-3 regulates protein kinase A modulation of the Ca(V)3.2 (alpha1H) T-type Ca^{2+} channels. *J Biol Chem* 2011; **286**: 2433–2444.
59. Markandeya YS, Phelan LJ, Woon MT, Keefe AM, Reynolds CR, August BK, Hacker TA, Roth DM, Patel HH, Balijepalli RC. Caveolin-3 overexpression attenuates cardiac hypertrophy via inhibition of T-type Ca^{2+} current modulated by protein kinase calpha in cardiomyocytes. *J Biol Chem* 2015; **290**:22085–22100.
60. Persson B, Argos P. Topology prediction of membrane proteins. *Protein Sci* 1996; **5**:363–371.
61. Krogh A, Larsson B, von Heijne G, Sonnhammer EL. Predicting transmembrane protein topology with a hidden markov model: application to complete. *J Mol Biol* 2001; **305**:567–580.
62. Song KS, Li S, Okamoto T, Quilliam LA, Sargiacomo M, Lisanti MP. Copurification and direct interaction of ras with caveolin, an integral membrane protein of caveolae microdomains. *J Biol Chem* 1996; **271**:9690–9697.
63. Zhang HH, Feng L, Livnat I, Hoh JK, Shim JY, Liao WX, Chen DB. Estradiol-17beta stimulates specific receptor and endogenous nitric oxide-dependent dynamic endothelial protein S-nitrosylation: analysis of endothelial nitrosyl-proteome. *Endocrinology* 2010; **151**:3874–3887.
64. Blizzard TA, Dininno F, Morgan JD, 2nd, Chen HY, Wu JY, Kim S, Chan W, Birzin ET, Yang YT, Pai LY, Fitzgerald PM, Sharma N et al. Estrogen receptor ligands. Part 9: Dihydrobenzoxathiin SERAMs with alkyl substituted pyrrolidine side chains and linkers. *Bioorg Med Chem Lett* 2005; **15**:107–113.
65. Chambliss KL, Yuhanna IS, Mineo C, Liu P, German Z, Sherman TS, Mendelsohn ME, Anderson RG, Shaul PW. Estrogen receptor alpha and endothelial nitric oxide synthase are organized into a functional signaling module in caveolae. *Circ Res* 2000; **87**:e44–e52.
66. Fujimoto T. Calcium pump of the plasma membrane is localized in caveolae. *J Cell Biol* 1993; **120**:1147–1157.
67. Rupnow HL, Phernetton TM, Shaw CE, Modrick ML, Bird IM, Magness RR. Endothelial vasodilator production by uterine and systemic arteries. VII. Estrogen and progesterone effects on eNOS. *Am J Physiol Heart Circ Physiol* 2001; **280**:H1699–H1705.
68. Magness RR, Rosenfeld CR. Local and systemic estradiol-17 beta: effects on uterine and systemic vasodilation. *Am J Physiol* 1989; **256**: E536–E542.
69. Scott PA, Tremblay A, Brochu M, St-Louis J. Vasorelaxant action of 17–estradiol in rat uterine arteries: role of nitric oxide synthases and estrogen receptors. *Am J Physiol Heart Circ Physiol* 2007; **293**: H3713–H3719.
70. Cruz MN, Agewall S, Schenck-Gustafsson K, Kublickiene K. Acute dilatation to phytoestrogens and estrogen receptor subtypes expression in small arteries from women with coronary heart disease. *Atherosclerosis* 2008; **196**:49–58.
71. Pedram A, Razandi M, Levin ER. Nature of functional estrogen receptors at the plasma membrane. *Mol Endocrinol* 2006; **20**:1996–2009.
72. Chambliss KL, Yuhanna IS, Anderson RG, Mendelsohn ME, Shaul PW. ERbeta has nongenomic action in caveolae. *Mol Endocrinol* 2002; **16**:938–946.
73. Batra S, Iosif S. Nuclear estrogen receptors in human uterine arteries. *Gynecol Obstet Invest* 1987; **24**:250–255.
74. Liu J, Garcia-Cardena G, Sessa WC. Palmitoylation of endothelial nitric oxide synthase is necessary for optimal stimulated release of nitric oxide: implications for caveolae localization. *Biochemistry* 1996; **35**:13277–13281.
75. Prabhakar P, Cheng V, Michel T. A chimeric transmembrane domain directs endothelial nitric-oxide synthase palmitoylation and targeting to plasmalemmal caveolae. *J Biol Chem* 2000; **275**:19416–19421.
76. Gabella G. Caveolae intracellulares and sarcoplasmic reticulum in smooth muscle. *J Cell Sci* 1971; **8**:601–609.
77. Kiss AL, Turi A, Mullner N, Kovacs E, Botos E, Greger A. Oestrogen-mediated tyrosine phosphorylation of caveolin-1 and its effect on the oestrogen receptor localisation: an in vivo study. *Mol Cell Endocrinol* 2005; **245**:128–137.
78. Haynes MP, Li L, Sinha D, Russell KS, Hisamoto K, Baron R, Collinge M, Sessa WC, Bender JR. Src kinase mediates phosphatidylinositol 3-kinase/Akt-dependent rapid endothelial nitric-oxide synthase activation by estrogen. *J Biol Chem* 2003; **278**:2118–2123.
79. Kim HP, Lee JY, Jeong JK, Bae SW, Lee HK, Jo I. Nongenomic stimulation of nitric oxide release by estrogen is mediated by estrogen receptor alpha localized in caveolae. *Biochem Biophys Res Commun* 1999; **263**: 257–262.
80. Li L, Haynes MP, Bender JR. Plasma membrane localization and function of the estrogen receptor alpha variant (ER46) in human endothelial cells. *Proc Natl Acad Sci USA* 2003; **100**:4807–4812.